

High-Mass Supersymmetry with High Energy Hadron Colliders

I. Hinchliffe*

Lawrence Berkeley National Laboratory, Berkeley, CA

F.E. Paige†

Brookhaven National Laboratory, Upton, NY

(Dated: November 10, 2018)

While it is natural for supersymmetric particles to be well within the mass range of the large hadron collider, it is possible that the sparticle masses could be very heavy. Signatures are examined at a very high energy hadron collider and an very high luminosity option for the Large Hadron Collider in such scenarios.

I. INTRODUCTION

If supersymmetry is connected to the hierarchy problem, it is expected [1] that sparticles will be sufficiently light that at least some of them will be observable at the Large Hadron Collider (LHC) or even at the Tevatron. However it is not possible to set a rigorous bound on the sparticle masses. As the sparticle masses rise, the fine tuning problem of the standard model reappears and the sparticle masses become large enough so that they are difficult to observe at LHC.

It is also possible that SUSY is also the solution to the dark matter problem [2], the stable, lightest supersymmetric particle (LSP) being the particle that pervades the universe. This constraint can be applied to the minimal SUGRA [3] model and used to constrain the masses of the other sparticles. Recently sets of parameters in the minimal SUGRA model have been proposed [4] that satisfy existing constraints, including the dark matter constraint and the one from the observed anomaly in the magnetic moment of the muon [5], but do not impose any fine tuning requirements. This set of points is not a random sampling of the available parameter space but is rather intended to illustrate the possible experimental consequences. These points and their mass spectra are shown in Table I. Most of the allowed parameter space corresponds to the case where the sparticles have masses less than 1 TeV or so and is accessible to LHC. Indeed some of these points are quite similar to ones studied in earlier LHC simulations [6] [7]. Points A, B, C, D, E, G, J and L fall into this category. As the masses of the sparticles are increased, the LSP contribution to dark matter rises and typically violates the experimental constraints. However there are certain regions of parameter space where the annihilation rates for the LSP can be increased and the relic density of LSP's lowered sufficiently. In these narrow regions, the sparticle masses can be much larger. Points F, K, H and M illustrate these regions. This paper considers Point K, H and M at the LHC with a luminosity upgrade to 1000 fb^{-1} per year, (SLHC) and at a possible higher energy hadron collider (VLHC). We assume an energy of 40 TeV for the VLHC and use the identical analysis for both machines. Point F has similar phenomenology to Point K except that the squark and slepton masses are much larger and consequently more difficult to observe. For the purposes of this simulation, the detector performance at $10^{35} \text{ cm}^{-2}\text{s}^{-1}$ and at the VLHC is assumed to be the same as that of ATLAS for at the LHC design luminosity. In particular, the additional pileup present at higher luminosity is taken into account only by raising some of the cuts. Isajet 7.54 [8] is used for the event generation. Backgrounds from $t\bar{t}$, gauge boson pairs, large p_T gauge boson production and QCD jets are included.

II. POINT K

Point K has $M_A \approx 2M_{\tilde{\chi}_1^0}$ and gluino and squark masses above 2 TeV. The strong production is dominated by valence squarks, which have the characteristic decays $\tilde{q}_L \rightarrow \tilde{\chi}_1^\pm q, \tilde{\chi}_2^0 q$ and $\tilde{q}_R \rightarrow \tilde{\chi}_1^0 q$. The signal can be observed in the inclusive effective mass distribution. Events are selected with hadronic jets and missing E_T and

*I.Hinchliffe@lbl.gov; The work was supported in part by the Director, Office of Energy Research, Office of High Energy and Nuclear Physics of the U.S. Department of Energy under Contract DE-AC03-76SF00098.

†paige@bnl.gov; The work was supported in part by the Director, Office of Energy Research, Office of High Energy and Nuclear Physics of the U.S. Department of Energy under Contract DE-AC02-98CH10886.

TABLE I: Benchmark SUGRA points and masses from Ref. [4]

Model	A	B	C	D	E	F	G	H	I	J	K	L	M
$m_{1/2}$	600	250	400	525	300	1000	375	1500	350	750	1150	450	1900
m_0	140	100	90	125	1500	3450	120	419	180	300	1000	350	1500
$\tan\beta$	5	10	10	10	10	10	20	20	35	35	35	50	50
$\text{sign}(\mu)$	+	+	+	-	+	+	+	+	+	+	-	+	+
$\alpha_s(m_Z)$	120	123	121	121	123	120	122	117	122	119	117	121	116
m_t	175	175	175	175	171	171	175	175	175	175	175	175	175
Masses													
h^0	114	112	115	115	112	115	116	121	116	120	118	118	123
H^0	884	382	577	737	1509	3495	520	1794	449	876	1071	491	1732
A^0	883	381	576	736	1509	3495	520	1794	449	876	1071	491	1732
H^\pm	887	389	582	741	1511	3496	526	1796	457	880	1075	499	1734
χ_1^0	252	98	164	221	119	434	153	664	143	321	506	188	855
χ_2^0	482	182	310	425	199	546	291	1274	271	617	976	360	1648
χ_3^0	759	345	517	654	255	548	486	1585	462	890	1270	585	2032
χ_4^0	774	364	533	661	318	887	501	1595	476	900	1278	597	2036
χ_1^\pm	482	181	310	425	194	537	291	1274	271	617	976	360	1648
χ_2^\pm	774	365	533	663	318	888	502	1596	478	901	1279	598	2036
\tilde{g}	1299	582	893	1148	697	2108	843	3026	792	1593	2363	994	3768
e_L, μ_L	431	204	290	379	1514	3512	286	1077	302	587	1257	466	1949
e_R, μ_R	271	145	182	239	1505	3471	192	705	228	415	1091	392	1661
ν_e, ν_μ	424	188	279	371	1512	3511	275	1074	292	582	1255	459	1947
τ_1	269	137	175	233	1492	3443	166	664	159	334	951	242	1198
τ_2	431	208	292	380	1508	3498	292	1067	313	579	1206	447	1778
ν_τ	424	187	279	370	1506	3497	271	1062	280	561	1199	417	1772
u_L, c_L	1199	547	828	1061	1615	3906	787	2771	752	1486	2360	978	3703
u_R, c_R	1148	528	797	1019	1606	3864	757	2637	724	1422	2267	943	3544
d_L, s_L	1202	553	832	1064	1617	3906	791	2772	756	1488	2361	981	3704
d_R, s_R	1141	527	793	1014	1606	3858	754	2617	721	1413	2254	939	3521
t_1	893	392	612	804	1029	2574	582	2117	550	1122	1739	714	2742
t_2	1141	571	813	1010	1363	3326	771	2545	728	1363	2017	894	3196
b_1	1098	501	759	973	1354	3319	711	2522	656	1316	1960	821	3156
b_2	1141	528	792	1009	1594	3832	750	2580	708	1368	2026	887	3216

the following scalar quantity formed

$$M_{eff} = \cancel{E}_T + \sum_{jets} E_{T,jet} + \sum_{leptons} E_{T,lepton}$$

where the sum runs over all jets with $E_T > 50$ GeV and $|\eta| < 5.0$ and isolated leptons with $E_T > 15$ GeV and $|\eta| < 2.5$. The following further selection was then made: events were selected with at least two jets with $p_T > 0.1M_{eff}$, $\cancel{E}_T > 0.3M_{eff}$, $\Delta\phi(j_0, \cancel{E}_T) < \pi - 0.2$, and $\Delta\phi(j_0, j_1) < 2\pi/3$. These cuts help to optimize the signal to background ratio. The distributions in M_{eff} for signal and background are shown in Figure 1. It can be seen that the signal emerges from the background at large values of M_{eff} . The LHC with 3000 fb^{-1} of integrated luminosity has a signal of 510 events on a background of 108 for $M_{eff} > 4000$ GeV. These rates are sufficiently large so that a discovery could be made with the standard integrated luminosity of 300 fb^{-1} . However the limited data samples available will restrict detailed studies.

Production of $\tilde{q}_R \tilde{q}_R$ followed by the decay of each squark to $q \tilde{\chi}_1^0$ gives a dijet signal accompanied by missing E_T . In order to extract this from the standard model background, hard cuts on the jets and \cancel{E}_T are needed. Events were required to have two jets with $p_T > 700$ GeV, $\cancel{E}_T > 600$ GeV, and $\Delta\phi(j_1, j_2) < 0.8\pi$. The resulting distributions are shown in Figure 2. Only a few events survive at the LHC with 3000 fb^{-1} . The transverse momentum of the hardest jet is sensitive to the \tilde{q}_R mass [7]. The mass determination will be limited by the available statistics.

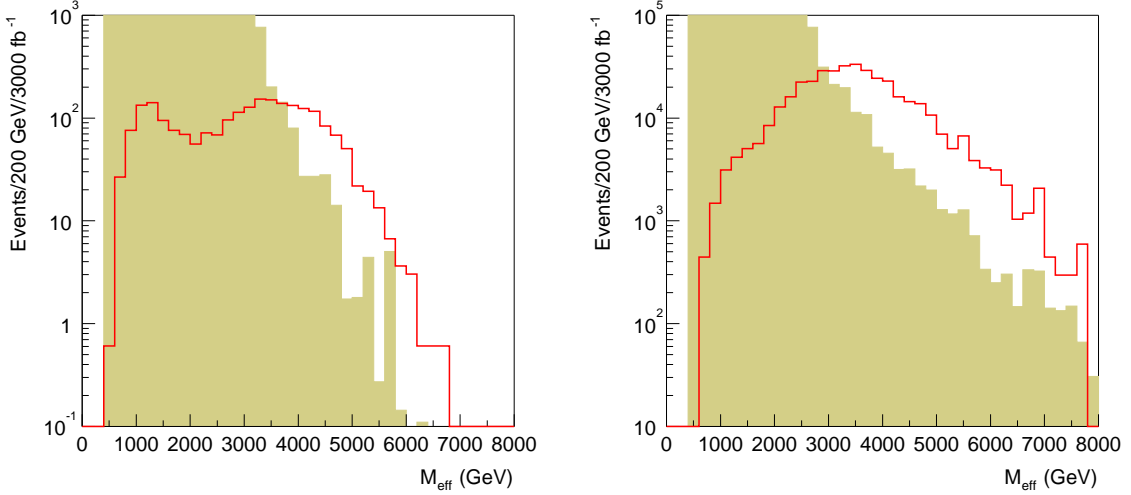


FIG. 1: M_{eff} distribution for SLHC (left) and VLHC (right) for Point K. Solid: signal. Shaded: SM background.

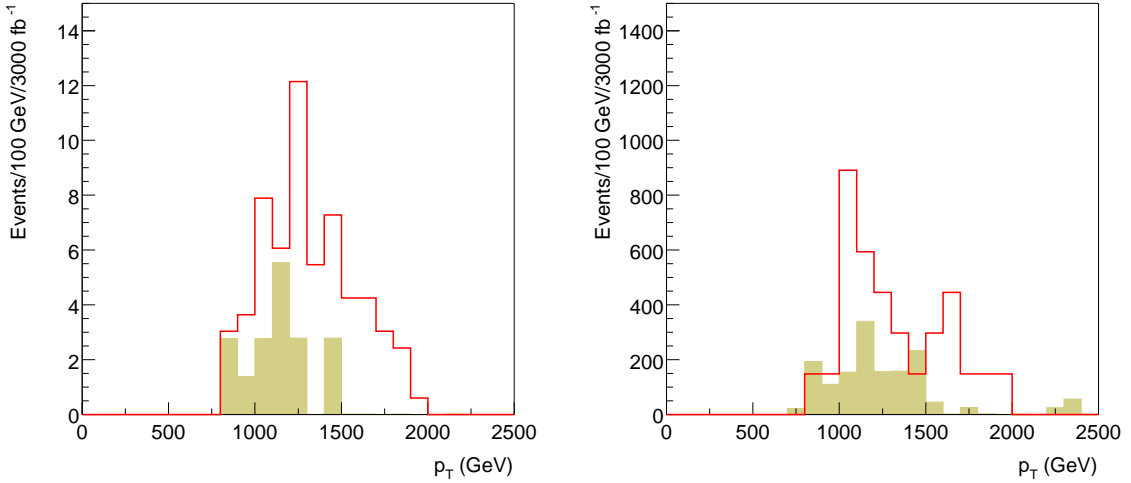


FIG. 2: p_T distribution of hardest jet in 2jet + \cancel{E}_T events for SLHC (left) and VLHC (right) for Point K.

The decay $\tilde{\chi}_2^0 \rightarrow \tilde{\chi}_1^0 h$ is dominant so we should expect to see Higgs particles in the decay of \tilde{q}_L ($\tilde{q}_L \rightarrow \tilde{\chi}_2^0 q \rightarrow \tilde{\chi}_1^0 h q$). The Higgs signal can be observed as a peak in the $b\bar{b}$ mass distributions. In order to do this, it is essential that b -jets can be tagged with good efficiency and excellent rejection against light quark jets. There is a large background from $t\bar{t}$ that must be overcome using topological cuts. Events were selected to have at least three jets with $p_T > 600, 300, 100$ GeV, $\cancel{E}_T > 400$ GeV, $M_{\text{eff}} > 2500$ GeV, $\Delta\phi(j_1, \cancel{E}_T) < 0.9\pi$, and $\Delta\phi(j_1, j_2) < 0.6\pi$. The distributions are shown in Figure 3 assuming the same b -tagging performance as for standard luminosity, *i.e.*, that shown in Figure 9-31 of Ref. [7] which corresponds to an efficiency of 60% and a rejection factor against light quark jets of ~ 100 . This b -tagging performance may be optimistic in the very high luminosity environment. However our event selection is only $\sim 10\%$ efficient at SLHC and might be improved. There is much less standard model background at VLHC. However, there is significant SUSY background from $\tilde{g} \rightarrow \tilde{b}_i \bar{b}, \tilde{t}_1 \bar{t}$ which becomes more important at the higher energy. At the VLHC and possibly at the SLHC, it should be possible to extract information on the mass of \tilde{q}_L by combining the Higgs with a jet and probing the decay chain $\tilde{q}_L \rightarrow \tilde{\chi}_2^0 q \rightarrow q h \tilde{\chi}_1^0$ (see e.g. [9]).

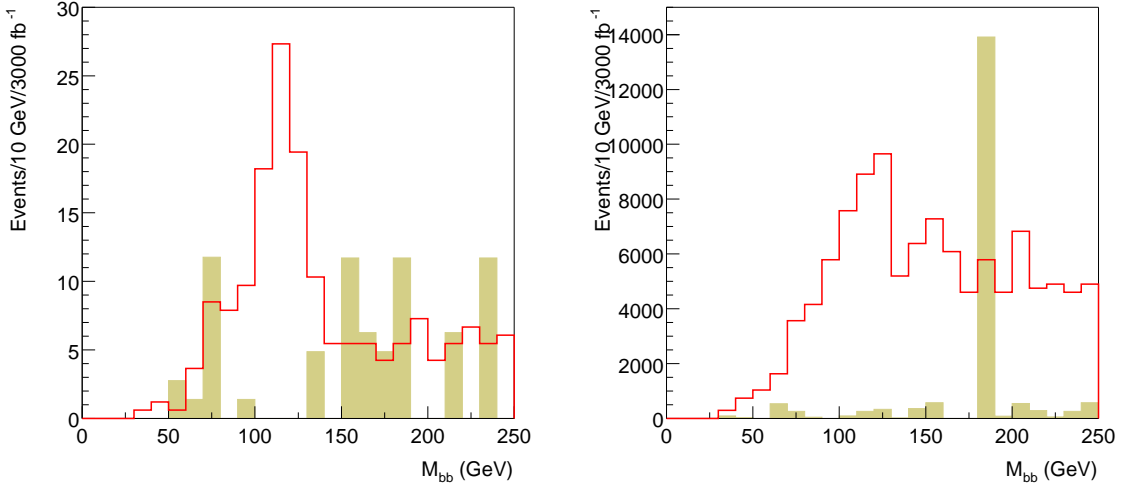


FIG. 3: M_{bb} distribution for SLHC (left) and VLHC (right) for Point K.

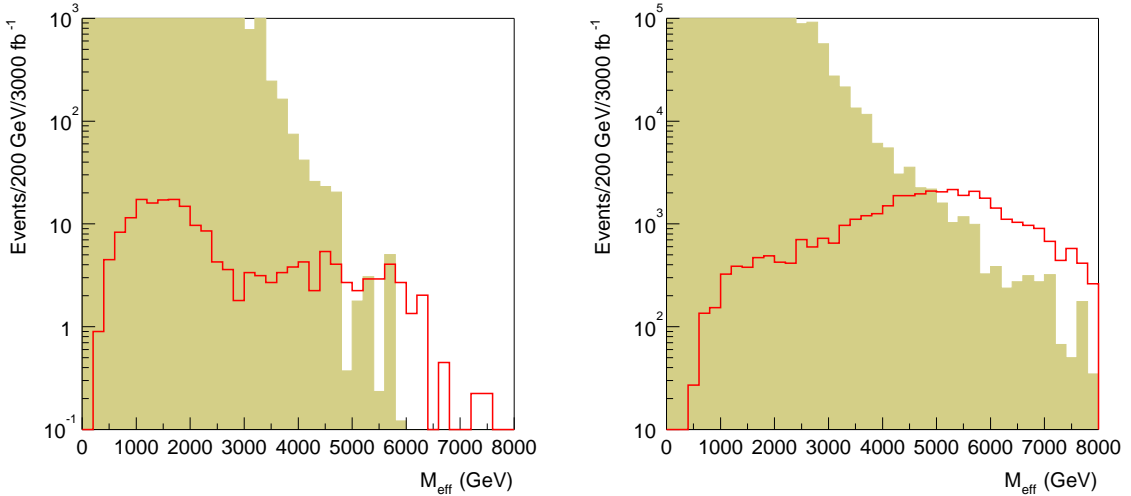


FIG. 4: M_{eff} distribution for SLHC (left) and VLHC (right) for Point M.

III. POINT M

Point M has squark and gluino masses around 3.5 TeV and is beyond the reach of the standard LHC. Only 375 SUSY events of all types are produced for 1000 fb^{-1} at LHC, mainly valence squarks ($\tilde{u}_L, \tilde{d}_L, \tilde{u}_R, \tilde{d}_R$) and gauginos ($\tilde{\chi}_1^\pm, \tilde{\chi}_2^0$). The VLHC cross section is a factor of 200 larger. About half of the SLHC SUSY events are from electro weak gaugino pair production mostly $\tilde{\chi}_2^0$ and $\tilde{\chi}_1^\pm$. The dominant decays of these are $\tilde{\chi}_2^0 \rightarrow \tilde{\chi}_1^0 h$ and $\tilde{\chi}_1^\pm \rightarrow \tilde{\chi}_1^0 W^\pm$. Rates are so small that no signal close to the Standard Model backgrounds could be found for the SLHC.

The effective mass distributions for Point M at SLHC and VLHC are shown in Figure 4 using the same cuts as for Point K. As expected, the SLHC signal is very marginal: there are only 20 signal events with 10 background events for $M_{eff} > 5000 \text{ GeV}$ and 3000 fb^{-1} . Several attempts to optimize the cuts did not give any improvement. Requiring a lepton, a hadronic τ , or a tagged b jet did not help. We are forced to conclude that it is unlikely that a signal of any type could be observed. The VLHC signal is clearly visible and could be further optimized.

The dilepton rates are shown in Fig 5. Events are selected that have $M_{eff} > 3000 \text{ GeV}$ $\cancel{E}_T > 0.2 M_{eff}$ and two isolated leptons with $p_T > 15 \text{ GeV}$ and the mass distribution of the dilepton pair shown. As expected, nothing is visible at SLHC. The distribution at VLHC is dominated by two independent decays (e.g. $\tilde{\chi}_1^\pm \tilde{\chi}_1^\mp \rightarrow \tilde{\chi}_1^0 \tilde{\chi}_1^0 W^\mp$),

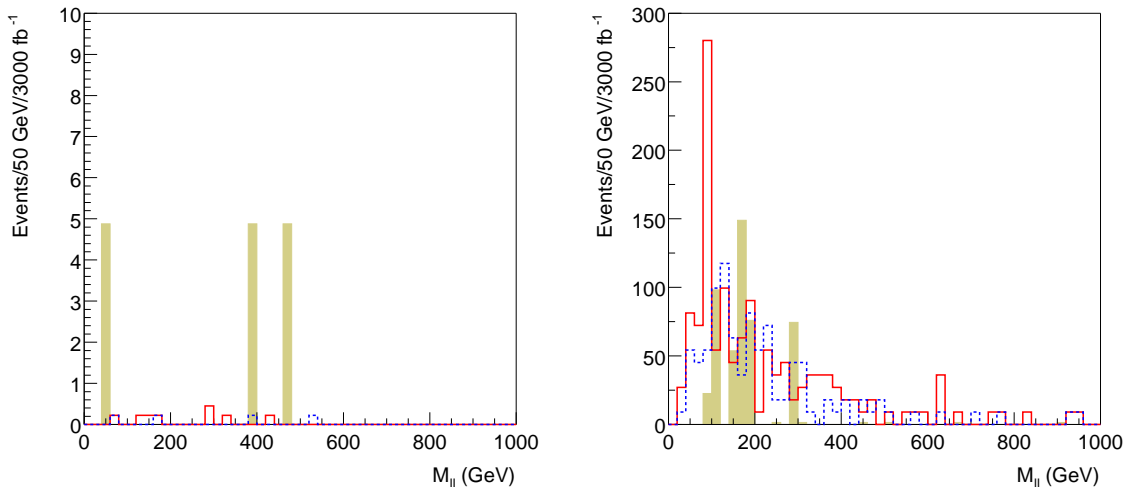


FIG. 5: Dilepton mass distribution for SLHC (left) and VLHC (right) for Point M. Solid: l^+l^- . Dashed: $e^\pm\mu^\mp$.

so that $e^+e^- + \mu^+\mu^-$ and $e^\pm\mu^\mp$ rates are almost identical except for the Z peak in the former which arises mainly from $\tilde{q} \rightarrow q\tilde{\chi}_2^\pm \rightarrow q\tilde{\chi}_1^\pm Z$.

On the basis of this preliminary study it seems unlikely that Point M can be detected at 14 TeV even with 3000 fb^{-1} . Higher energy would be required.

IV. POINT H

Point H is able to accommodate very heavy sparticles without overclosing the universe as the destruction rate for the $\tilde{\chi}_1^0$ is enhanced by coannihilation with a stau. This implies a very small splitting between the $\tilde{\tau}_1$ and the $\tilde{\chi}_1^0$. In this particular case, $\tilde{\tau}_1 \not\rightarrow \tilde{\chi}_1^0\tau$, so it must decay by second order weak processes, $\tilde{\tau}_1 \rightarrow \tilde{\chi}_1^0 e\bar{\nu}_e\nu_\tau$, giving it a long lifetime. The dominant SUSY rates arise from the strong production of valance squarks, with $\tilde{q}_L \rightarrow \tilde{\chi}_1^\pm q$, $\tilde{\chi}_2^0 q$ and $\tilde{q}_R \rightarrow \tilde{\chi}_1^0$. The stau which are produced from cascade decays of these squarks, then exit the detector with a signal similar to a ‘‘heavy muon’’.

The p_T spectrum of these quasi-stable $\tilde{\tau}_1$ for 1000 fb^{-1} is shown in Figure 6. The ATLAS muon system [7] has a time resolution of about 0.7 ns for time of flight over a cylinder of radius 10 m and half-length 20 m. The spectrum with a time delay $\Delta t > 10\sigma$ (7 ns) is also shown. Notice that this signal could be observed at the LHC with $\sim 300 \text{ fb}^{-1}$. Triggering on a slow $\tilde{\tau}_1$ may be a problem since the time-window for the trigger chambers is limited. However, the \cancel{E}_T in SUSY events as measured by the calorimeter is quite large as shown in Figure 7. It probably is possible to trigger just on jets plus \cancel{E}_T , the distribution for which is shown in Figure 7. The mass of the stable stau can be measured by exploiting the time of flight measurements in the muon measurement system. Studies of such quasi stable particles at somewhat smaller masses carried out on the ATLAS detector showed a mass resolution of approximately 3% given sufficient statistics (see Section 20.3.4.2 of Ref [7]). A precision of this order should be achievable with 3000 fb^{-1} at either the LHC or VLHC. One can then build on the stable stau to reconstruct the decay chain using techniques similar to those used for the GMSB studies [7] [10]. This is not pursued here.

The stable τ_1 signature is somewhat exceptional so we explore other signatures that do not require it and would be present if the stau decayed inside the detector. For such high masses the strong production is mainly of \tilde{u} and \tilde{d} . Events are selected with hadronic jets and missing E_T and the effective mass formed as in the case of Point K. To optimize this signature, events were further selected with at least two jets with $p_T > 0.1M_{\text{eff}}$, $\cancel{E}_T > 0.3M_{\text{eff}}$, $\Delta\phi(j_0, \cancel{E}_T) < \pi - 0.2$, and $\Delta\phi(j_0, j_1) < 2\pi/3$. The M_{eff} distributions after these cuts for the SLHC and the VLHC are shown in Fig 8. Note that at the SLHC the number of events in the region where $S/B > 1$ is very small. Given the uncertainties in the modeling of the standard model backgrounds the shower Monte Carlo, it is not possible to claim that the SLHC could see a signal using this global variable. The VLHC should have no difficulty as there are several thousand events for $M_{\text{eff}} > 5 \text{ TeV}$.

Dileptons arise from the cascade $\tilde{q}_L \rightarrow q\tilde{\chi}_2^0 \rightarrow q\ell^+\ell^-\tilde{\chi}_1^0$. The dilepton mass distributions should have a kinematic endpoint corresponding to this decay. Figure 9 shows the distribution for same flavor and different

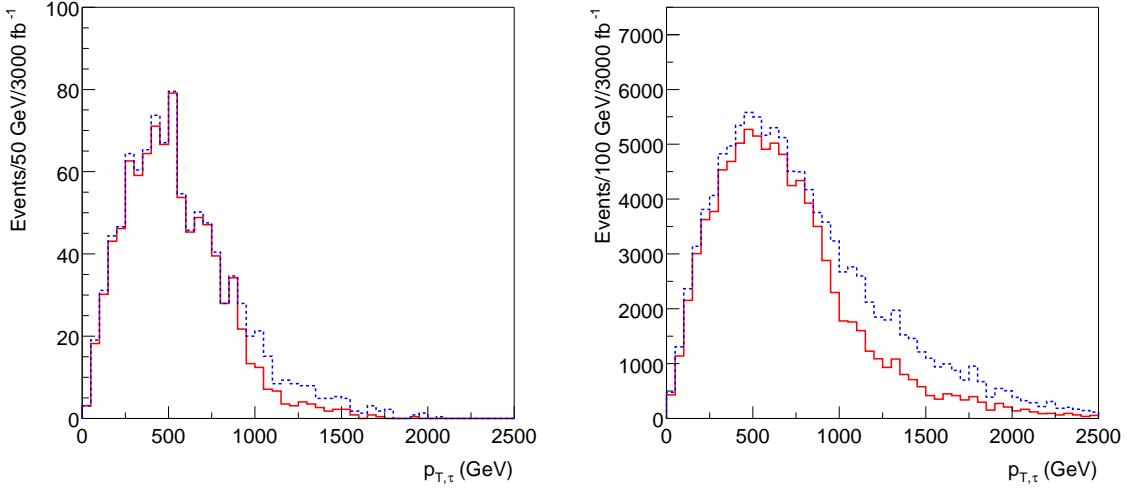


FIG. 6: p_T distribution of $\tilde{\tau}_1$ at SLHC (left) and VLHC (right) for Point H. Dashed: all $\tilde{\tau}_1$. Solid: $\tilde{\tau}_1$ with $\Delta t > 7$ ns

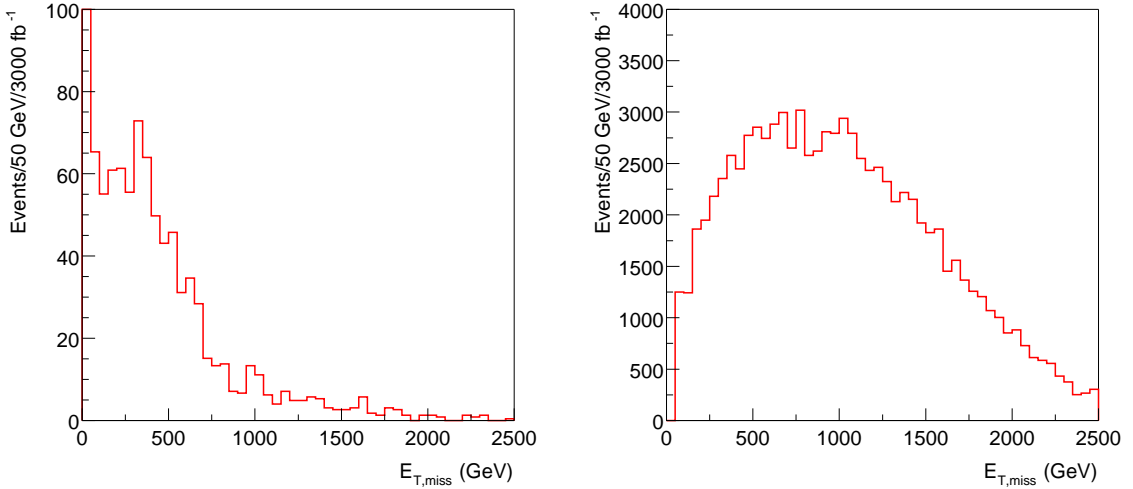


FIG. 7: Calorimetric \cancel{E}_T distributions in $\tilde{\tau}_1$ events for SLHC (left) and VLHC (right) for Point H.

flavor lepton pairs. Events were required to have $M_{\text{eff}} > 3000$ GeV and $\cancel{E}_T > 0.2M_{\text{eff}}$ and to have two isolated opposite sign leptons with $E_T > 15$ GeV and $|\eta| < 2.5$. The structure at the VLHC is clear; the edge comes mainly from $\tilde{\chi}_2^0 \rightarrow \tilde{\ell}_L^\pm \ell^\mp$, which has a branching ratio of 15% per flavor. This gives an endpoint at

$$\sqrt{\frac{(M_{\tilde{\chi}_2^0}^2 - M_{\tilde{\ell}_L}^2)(M_{\tilde{\ell}_L}^2 - M_{\tilde{\chi}_1^0}^2)}{M_{\tilde{\ell}_L}^2}} = 447.3 \text{ GeV}$$

consistent with the observed endpoint in Figure 9. Of course this plot does not distinguish $\tilde{\ell}_L$ and $\tilde{\ell}_R$. In the case of the upgraded LHC, the signal may be observable, but it should be noted that the background is uncertain as only three generated events passed the cuts.

If the stable stau is used then the situation improves considerably. The dilepton mass for events containing a $\tilde{\tau}_1$ with a time delay $7 < \Delta t < 21.5$ ns is shown in Figure 10. Since $\Delta t > 10\sigma$, the standard model background is expected to be negligible. The SLHC signal is improved and a measurement should be possible. The acceptance for VLHC is somewhat worse than the inclusive sample, but having the correlation of the dileptons with the $\tilde{\tau}_1$ should be useful.

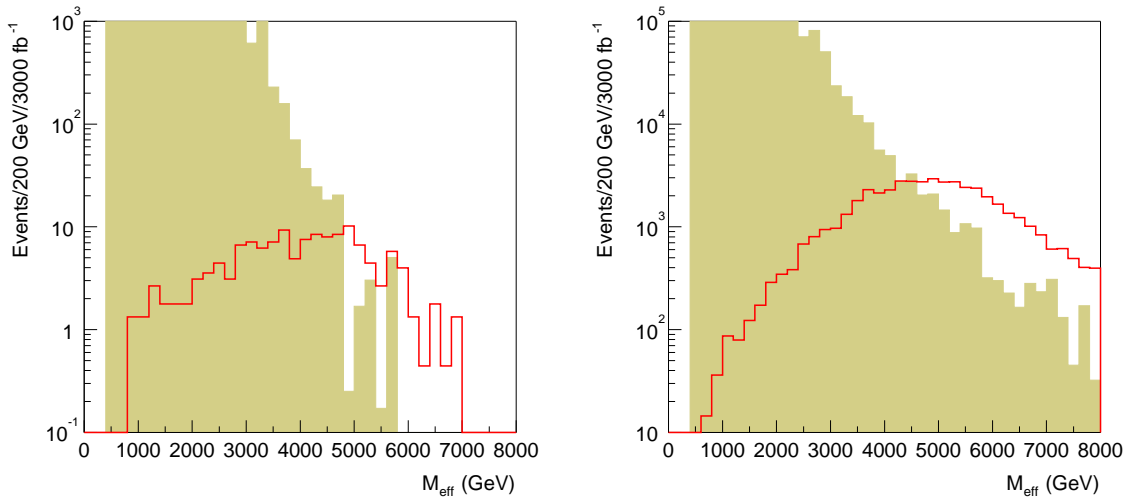


FIG. 8: M_{eff} distribution for SLHC (left) and VLHC (right) for Point H. Solid: signal. Shaded: SM background.

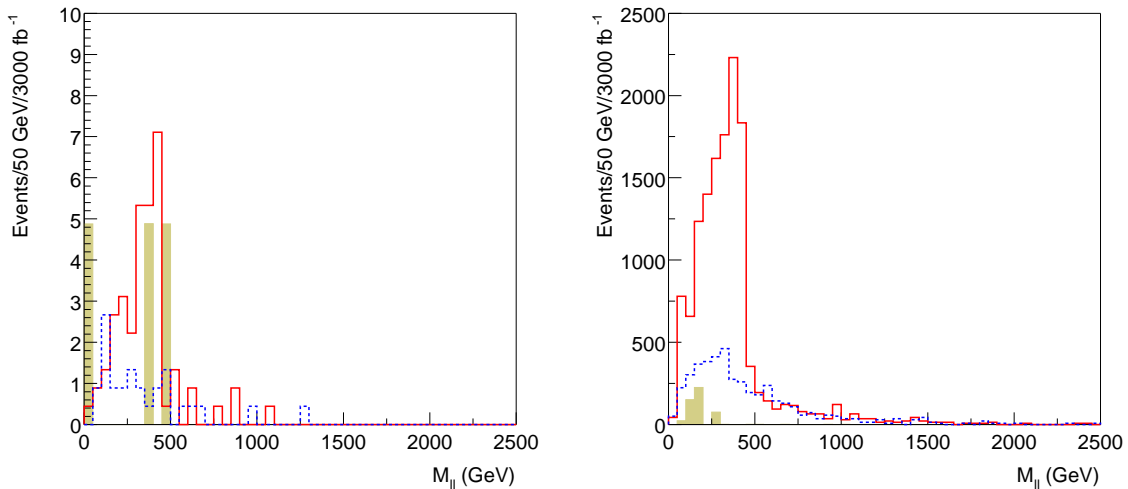


FIG. 9: $M_{\ell\ell}$ distribution for SLHC (left) and VLHC (right) for Point H. Solid: $\ell^+\ell^-$. Dashed: $e^\pm\mu^\mp$.

The VLHC gives a gain of ~ 100 in statistics over the LHC for the same luminosity at this point, which is at the limit of observability at the LHC. If the VLHC luminosity were substantially lower, the improvement provided by it would be rather marginal. The cross section increases by another factor of ~ 100 at 200 TeV.

V. CONCLUSIONS

We have surveyed the signals at hadron colliders for the SUGRA models proposed by [4] concentrating on the cases where the sparticle masses are very large. While the masses of the sparticles at Point K are such that SUSY would be discovered at the baseline LHC, the event rates are small and detailed SUSY studies will not be possible. The reach of the LHC for would be improved by higher luminosity where the extraction of specific final states will become possible. The cross section at a 40 TeV VLHC is approximately 100 times larger than that at LHC. This leads to a substantial gain, but it is important to emphasize that this gain requires luminosity at least as large as that ultimately reached by the LHC and detectors capable of exploiting it. Point H has a special feature in that the stau is quasi-stable. This feature would enable a signal to be extracted at SLHC. If the tau mass were raised slightly so that its lifetime were short, then only the VLHC could observe it.

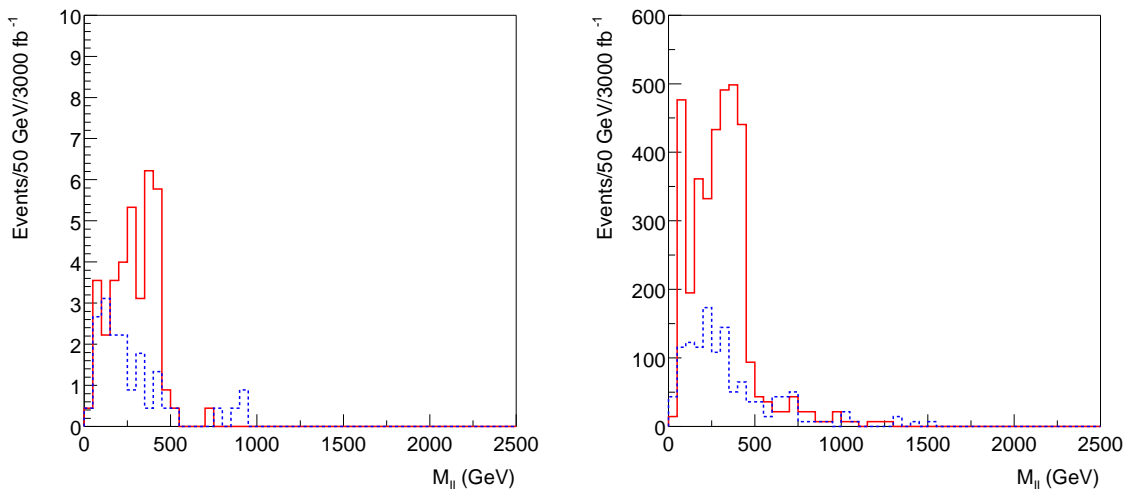


FIG. 10: $M_{\ell\ell}$ distribution for SLHC (left) and VLHC (right) for events containing a $\tilde{\tau}_1$ for Point H. Solid: $\ell^+\ell^-$. Dashed: $e^\pm\mu^\mp$.

The masses in the case of Point M are so large that the VLHC would be required for discovery. Point F has a gluino mass of order 2 TeV and should be observable at the LHC exploiting the production of gluinos followed by the decays to $\tilde{\chi}_i$ and hence to leptons.

The Points A, B, C, D, G, I, and L which are much less fine tuned have similar phenomenology to the “Point 5” or “Point 6” analysis of [7] in that lepton structure from the decay $\tilde{\chi}_2^0 \rightarrow \tilde{\ell}_R \ell \rightarrow \ell^+\ell^-\tilde{\chi}_1^0$ and/or $\tilde{\chi}_2^0 \rightarrow t\tilde{u}\tau \rightarrow \tau^+\tau^-\tilde{\chi}_1^0$ is present. In most cases decay $\tilde{\chi}_2^0 \rightarrow \tilde{\ell}_L \ell$ is also allowed, so that a more complicated dilepton mass spectrum is observable. This should enable the extraction of m_{ℓ_L} in addition (for an example see Fig 20-53 of [7]). Points A, D and L have higher squark/gluino masses and will require more integrated luminosity. Nevertheless one can have confidence that the baseline LHC will make many measurements in all of these cases.

The work was supported in part by the Director, Office of Energy Research, Office of High Energy and Nuclear Physics of the U.S. Department of Energy under Contracts DE-AC03-76SF00098 and DE-AC02-98CH10886. Accordingly, the U.S. Government retains a nonexclusive, royalty-free license to publish or reproduce the published form of this contribution, or allow others to do so, for U.S. Government purposes.

-
- [1] G. W. Anderson and D. J. Castano, Phys. Lett. B **347**, 300 (1995). R. Barbieri and G. F. Giudice, Nucl. Phys. B **306**, 63 (1988).
- [2] J. Ellis, *et al.*, Nucl. Phys. **B238**, 453 (1984);
A. Gabutti *et al.*, hep-ph/9602432;
H. Baer and M. Brhlik, Phys. Rev. **D53**, 597 (1996).
- [3] L. Alvarez-Gaume, J. Polchinski and M.B. Wise, Nucl. Phys. **B221**, 495 (1983); L. Ibañez, Phys. Lett. **118B**, 73 (1982); J.Ellis, D.V. Nanopolous and K. Tamvakis, Phys. Lett. **121B**, 123 (1983); K. Inoue *et al.* Prog. Theor. Phys. **68**, 927 (1982); A.H. Chamseddine, R. Arnowitt, and P. Nath, Phys. Rev. Lett., **49**, 970 (1982).
- [4] M. Battaglia *et al.*, hep-ph/0106204.
- [5] H. N. Brown *et al.* [Muon g-2 Collaboration], Phys. Rev. Lett. **86**, 2227 (2001)
- [6] S. Abdullin *et al.* [CMS Collaboration], “Discovery potential for supersymmetry in CMS,” hep-ph/9806366.
- [7] ATLAS Collaboration, *ATLAS Detector and Physics Performance Technical Design Report*, CERN/LHCC/99-14, <http://atlasinfo.cern.ch/Atlas/GROUPS/PHYSICS/TDR/access.html>.
- [8] F. Paige and S. Protopopescu, in *Supercollider Physics*, p. 41, ed. D. Soper (World Scientific, 1986);
H. Baer, F. Paige, S. Protopopescu and X. Tata, in *Proceedings of the Workshop on Physics at Current Accelerators and Supercolliders*, ed. J. Hewett, A. White and D. Zeppenfeld, (Argonne National Laboratory, 1993).
- [9] I. Hinchliffe, F. E. Paige, M. D. Shapiro, J. Soderqvist and W. Yao, Phys. Rev. D **55**, 5520 (1997)
- [10] I. Hinchliffe and F. E. Paige, Phys. Rev. D **60**, 095002 (1999)